Plant Mol Biol (2007) 63:787–801
DOI 10.1007/s11103-006-9126-7

Putrescine *N*-methyltransferases—a structure–function analysis

Michael Teuber · Mohammad E. Azemi · Foroogh Namjoyan · Anna-Carolin Meier · Anja Wodak · Wolfgang Brandt · Birgit Dräger

Received: 3 October 2006 / Accepted: 14 December 2006 / Published online: 14 January 2007

Abstract Putrescine *N*-methyltransferase (PMT) is a key enzyme of plant secondary metabolism at the start of the specific biosynthesis of nicotine, of tropane alkaloids, and of calystegines that are glycosidase inhibitors with nortropane structure. PMT is assumed to have developed from spermidine synthases (SPDS) participating in ubiquitous polyamine metabolism. In this study decisive differences between both enzyme families are elucidated. PMT sequences were known from four Solanaceae genera only, therefore additional eight PMT cDNA sequences were cloned from five Solanaceae and a Convolvulaceae. The encoded polypeptides displayed between 76% and 97% identity and typical amino acids different from plant spermidine synthase protein sequences. Heterologous expression of all enzymes proved catalytic activity exclusively as PMT and K_{cat} values between 0.16 s^{-1} and 0.39 s^{-1}. The active site of PMT was initially inferred from a protein structure of spermidine synthase obtained by protein crystallisation. Those amino acids of the active site that were continuously different between PMTs and SPDS were mutated in one of the PMT sequences with the idea of changing PMT activity into spermidine synthase. Mutagenesis of active site residues unexpectedly resulted in a complete loss of catalytic activity. A protein model of PMT was based on the crystal structure of SPDS and suggests that overall protein folds are comparable. The respective cosubstrates *S*-adenosylmethionine and decarboxylated *S*-adenosylmethionine, however, appear to bind differentially to the active sites of both enzymes, and the substrate putrescine adopts a different position.

Keywords Calystegines · Convolvulaceae · Putrescine *N*-methyltransferase · Solanaceae · Spermidine synthase · Tropane alkaloids

Abbreviations

AdoDATO	*S*-adenosyl-1,8-diamino-3-thiooctane
dcSAM	Decarboxylated *S*-adenosylmethionine
PMT	Putrescine *N*-methyltransferase
SAM	*S*-adenosylmethionine
SPDS	Spermidine synthases
bp	Base pairs

Introduction

Methyltransferases possess essential biological functions in nucleic acid methylation and protein methylation, which alters DNA, RNA, or protein activity or function. Methylation of small molecules such as mammalian and plant hormones or plant secondary metabolites is of equivalent importance for the respective organism. Putrescine *N*-methyltransferase (PMT) is the first pathway-specific enzyme in the biosynthesis of nicotine, of the tropane alkaloids atropine,

M. Teuber · M. E. Azemi · F. Namjoyan · A.-C. Meier · A. Wodak · B. Dräger (✉)
Institute of Pharmacy, Faculty of Science I,
Martin-Luther University Halle-Wittenberg,
Hoher Weg 8, 06120 Halle/Saale, Germany
e-mail: birgit.draeger@pharmazie.uni-halle.de

W. Brandt
Department of Bioorganic Chemistry,
Leibniz Institute of Plant Biochemistry,
Weinberg 3, 06120 Halle/Saale, Germany

scopolamine, and cocaine, and of calystegines (Fig. 1). Calystegines are polyhydroxyl alkaloids with strong glycosidase inhibitory activity. They occur more widespread in the plant kingdom than assumed before for the distribution of tropane alkaloids (Lounasmaa and Tamminen 1993; Griffin and Lin 2000); Brassicaceae (Brock et al. 2006) and Moraceae (Asano et al. 1994a, b) contain calystegines.

The first PMT cDNA sequence was obtained by subtractive hybridisation on cDNA banks exploiting different transcript levels between tobacco cultivars rich and poor in nicotine (Hibi et al. 1994). Further PMT cDNA sequences from *Nicotiana* species were found screening genomic DNA libraries by 5′-terminal PMT-fragments as probes (Riechers and Timko 1999; Winz and Baldwin 2001) that contain 33 base pairs repeated two to nine times (Hashimoto et al. 1998a).

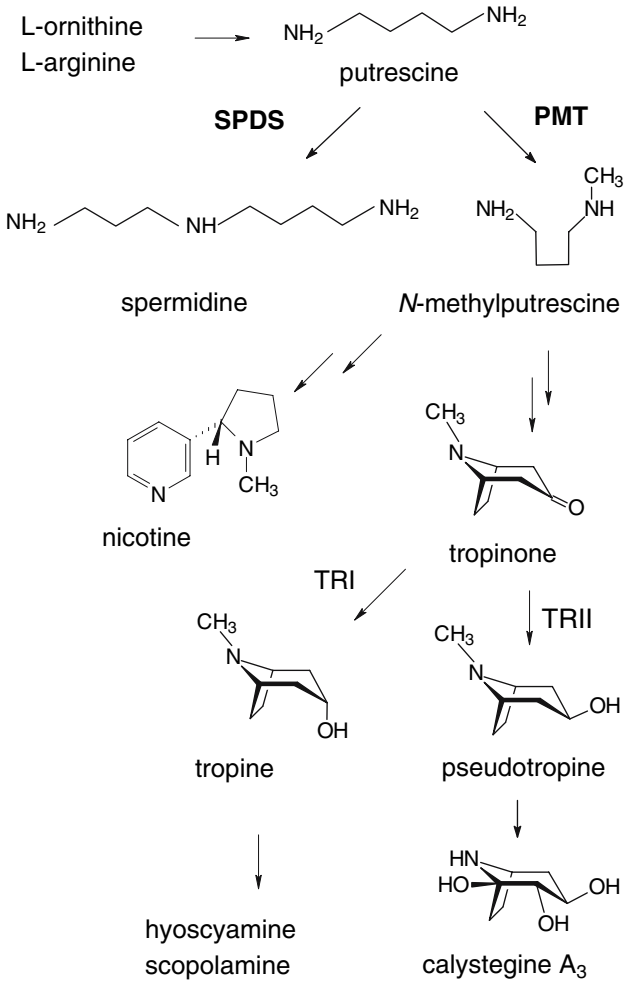

Fig. 1 Biosynthesis of nicotine and of tropane derived alkaloids catalysed by putrescine *N*-methyltransferase (PMT). SPDS spermidine synthase, TRI tropine forming tropinone reductase TRII pseudotropine forming tropinone reductase

For PMT cloning from *Hyoscyamus niger* and *Atropa belladonna*, cDNA libraries from roots were screened with full length tobacco PMT probes (Hashimoto et al. 1998b; Suzuki et al. 1999).

Spermidine synthases (SPDS) accept putrescine, the same substrate as PMT, but a slightly different cosubstrate, decarboxylated *S*-adenosylmethionine (dcSAM), and they show high sequence similarity to PMT. In fact, cloning of a plant spermidine synthase was a fortuitous result when screening for PMT (Hashimoto et al. 1998a). Similarly, screening a cDNA library from potato sprouts for PMT produced potato SPDS sequences (Stenzel et al. 2006). The homology of PMT and plant SPDS, e.g., 67% for *H. niger*, renders rapid and reliable PCR amplification of *pmt*-coding sequences difficult, when no *N*-terminal repeat typical for *Nicotiana pmts* is present in the coding sequence. From *Anisodus tanguticus* (Solanaceae) a full-length *pmt* sequence was cloned recently starting from a 578 bp (base pair) PCR-fragment completed by nested RACE-PCR (Liu et al. 2005). No information was given whether this strategy also yielded SPDS sequences. Extensive alignments of *S*-adenosylmethionine (SAM)-dependent methyltransferases of various origins and activities (Kagan and Clarke 1994; Schluckebier et al. 1995; Kozbial and Mushegian 2005) and of small molecule methyltransferases from plants in particular (Joshi and Chiang 1998) revealed a high degree of sequence variability, yet conserved motifs were postulated to participate in SAM binding. All motifs described for methyltransferases show no or little conservation in PMTs, which renders them insufficient for a sequence-based distinction between *pmt* and *spds*.

Similarity between SPDS and PMT sustained the hypothesis that specific PMT sequences have evolved from plant SPDS (Hashimoto et al. 1998a). The concept of gene duplication and mutation of one gene copy until a change of function or specification of function is achieved, is well supported by evidence, however, the process of step-by-step mutation is poorly illustrated. PMT sequences form an excellent model to study the constraints and the necessities for evolution of a new function from the ubiquitous coding sequence of SPDS. The enzyme kinetics probably developed during evolution from uni-uni-ping-pong for SPDS (Yoon et al. 2000) to ordered bi-bi for PMT (Hibi et al. 1992; Walton et al. 1994). The identification of conserved residues and of decisive alterations in SPDS genes and proteins that changed catalytic function from SPDS to PMT requires an array of PMT sequences demonstrating their natural variation. The difficulties in *pmt* cloning mentioned above may have

limited published *pmt* sequences to those from four related Solanaceae genera. Therefore, selective PCR-based cloning of eight *pmt* sequences with appropriate primers and confirmation of the identity by protein expression and enzyme activity was the first step of the study of PMT natural variation.

Plants were chosen with the aim to provide a variety of PMTs and to test the PCR strategy. Root cultures of *Datura innoxia* and *D. stramonium* were expected to contain *pmt* transcripts, because they synthesise tropane alkaloids, and the enzyme was purified from *D. stramonium* (Walton et al. 1994). In leaves of *Solanum dulcamara*, calystegine B_2 had been detected (Nash et al. 1993). *Physalis divaricata* was not investigated for tropane alkaloids before, but other *Physalis* species contain calystegines or tropane alkaloids, i.e., tigloidine in *P. peruviana* (Yamaguchi and Nishimoto 1965) and in *P. alkekengi* (Beresford and Woolley 1974) and calystegines in *P. alkekengi* (Asano et al. 1995). Tomato was included in the search as calystegines were described in fruits (Asano et al. 1997). *Calystegia sepium*, eponymous for calystegines, was included, because it belongs to a different plant family, Convolvulaceae (Scholl et al. 2001). Sufficient similarity of *pmt* for primer annealing and PCR amplification was therefore uncertain.

Four sequence motifs were selected as typical for PMT and different from SPDS sequences. Considerable overall sequence similarity between plant SPDS and PMT offered the opportunity to study the impact of individual amino acids on catalysis and suggested to try the conversion of PMT activity to SPDS by equivalent exchanges. Thus individual amino acid residues that differed typically between SPDS and PMT on enzymatic function were exchanged by site-directed mutagenesis.

Materials and methods

Plant material

Seeds of *Physalis divaricata* were collected in Fars, Iran, and authenticated with the help of Dr. B. Zehzad, Biology Department of Shahid Beheshti University of Science, Teheran. Seeds of *Calystegia sepium* and of *Solanum dulcamara* were collected in Halle, Germany, and authenticated by Dr. M. H. Hoffmann, Botanic Institute of Martin Luther University. Seeds of *Datura innoxia* and *D. stramonium* were obtained from the Botanic Garden of Martin Luther University. Seeds of tomato, *Lycopersicum esculentum* (syn. *Solanum lycopersicon*) *cv*. Moneymaker were obtained from N.L. Chrestensen, Samen- und Pflanzenzucht GmbH (Erfurt, Germany). Voucher specimens are deposited at the Department of Pharmacognosy, Faculty of Pharmacy, Shaheed Beheshti University, and at the Institute of Pharmacy, Martin Luther University, respectively. Seeds were germinated, and plants were grown in pots (24 cm diameter) on commercial potting, soil either outside or in a greenhouse at 22–25°C, 50% humidity and 18 h light. Root cultures of the plants used in this study were established from seedlings grown from sterilised seeds (sodium hypochlorite 5% and sodium dodecylsulphate 0.5% in water, 10 min) on agar containing B5 salts (Gamborg et al. 1968). When roots had developed on the seedlings after 3–5 weeks in glass containers with permanent illumination at 22°C, they were cut off by a sterile blade and transferred into liquid B5 medium containing 1 μM idole-3-butyric acid and 3% sucrose. Roots were sub-cultured after 21 days into 70 ml B5 medium in 300 ml flasks on a gyrotary shaker (100 strokes/min) and kept dark.

Cloning of pmt, spds and β-amylase

Putrescine *N*-methyltransferase cloning was done from mRNA of roots cut from intact plants (3 g fresh mass per sample). For mRNA extraction roots were collected, rinsed intensively by tap water (5 min), and quickly frozen in liquid nitrogen. Total RNA was extracted from plant tissues by phenol and chloroform (Sambrook et al. 1989). Internal fragments of *pmt* were obtained after RT-PCR on mRNA (Superscript II, Invitrogen) with the primer combinations *pmt*-fwd-A and *pmt*-rev-A or *pmt*-fwd-B and *pmt*-rev-B (Table 1) using *Taq*-Polymerase (peqGOLD Taq-DNA-Polymerase, peqlab Biotechnology, Erlangen, Germany). After sequencing internal fragments were completed by RACE-PCR (5′-RACE system, 3′-RACE System version 2; both Invitrogen). Full length cDNAs were obtained by gene-specific primers (Table 1), ligated into vector pCR2.1-TOPO (Invitrogen) and sequenced for control. Full-length *spds* cDNA was obtained from *D. stramonium* and *L. esculentum* mRNA after RT-PCR with gene specific primers and *Pfu*-Polymerase (*PfuUltra* High-Fidelity DNA Polymerase, Stratagene), ligated into pCR2.1-TOPO and sequenced for control. A fragment of the *C. sepium* β-amylase gene was obtained similarily from cDNA by PCR with *Taq* polymerase, ligated into pCR2.1-TOPO and sequenced for control.

Protein expression

After cloning of the sequences into vector pET21d (Merck Biosciences), plasmids were transferred into

Table 1 PCR primers (all in 5′ → 3′ direction)

Primers for initial *pmt* fragment	
pmt-fwd-A	AATGGTGGATTTCCATACAC
pmt-rev-A	GCTGCTTTGTGAATATCAGAG
pmt-fwd-B	AATGGTGGATTTCCATATAC
pmt-rev-B	GCTGCTTTATGAATATCAGAG
Primers for full length clones (restriction sites underlined)	
Cs-*pmt1*-fwd-*Nco*I	CCATGGAGGTCATGGCTGCTC
Cs-*pmt2*-fwd-*Nco*I	CCATGGGCCACGACAATGGCAACAAGT
Cs-*pmt*-rev-*Xho*I	CTCGAGCTCGAGCAATTTTTGCACAAAGG
Di-*pmt*-fwd-*Nco*I	CCATGGAAGTCATATCCACTC
Di-*pmt*1-rev-*Xho*I	CTCGAGAGACTCTATCATACTTCTGG
Di-*pmt*2-rev-*Xho*I	CTCGAGAGACTCAGTCAGATTTTTGG
Ds-*pmt*-fwd-*Nco*I	CCATGGAAGTCTTGTCATCTACCCAC
Ds-*pmt*-rev-*Xho*I	CTCGAGAGACTCTATCATACTTCTGGCAAAAG
Le-*pmt*-fwd-*Nco*I	CCATGGAGGTCATAATGAACAATCACAAC
Le-*pmt*-rev-*Xho*I	CTCGAGAGATTCAAACAAATCCCTTGCAAAAG
Pd-*pmt*-fwd-*Nco*I	CCATGGAAGTCATGACATCTACCCAC
Pd-*pmt*-rev-*Xho*I	CTCGAGAGACTCAATCAAACTTGCAGCAAAAG
Sd-*pmt*-fwd-*Nco*I	CCATGGAAGTCATATCTAATCACA
Sd-*pmt*-rev-*Xho*I	CTCGAGAGACTCAATCAAACTTCTGGG
Ds-*spds*1-fwd	ATGGAAGAAGCCAATAACAAAGAATCTCC
Ds-*spds*1-rev	GAGGGTGATTGAATCCAAAGGAAAATGA
Le-*spds*-fwd	ATGGCAGATGAGTGTGCTGCTTTTATG
Le-*spds*-rev	GAGGGTGATCGAAACCAAAGGAAAATAA
Primers for amplification of Northern blot probes	
Ds-*pmt-fwd*-probe	TGGAAGTCTTGTCATCTACCCAC
Ds-*pmt*-rev-probe	CCTGGCCATAAGGCGCTAAAC
Le-*pmt*-fwd-probe	ATGGAGGTCATAATGAACAATCACAAC
Le-*pmt*-rev-probe	TGATAGAGTTAGTGAACTCTACAAGC
Cs-pmt-fwd-probe	ATGGAGGTCATGGCTGCTCACAATAATG
Cs-*pmt*-rev-probe	ACCCCGGCTTAATGCACCCAAAG
Primers for RT-PCR control of *C. sepium* β-amylase 589 bp fragment	
Cs-*amyl*-fwd	CCCTGTCTATGTAATGCTCC
Cs-*amyl*-rev	GGTATTGGAGAATTTCAGTGC
Primers for mutagenesis (*D. stramonium*)	
pmt-I141D-fwd	AGGTTTTGATCATTGGTGGAGGAGATGGTTTTACATTATTCG
pmt-I141D-rev	TCGAATAATGTAAAACCATCTCCTCCACCAATGATCAAAACC
pmt-I136V-fwd	ATCCAAAAAAGGTTTTGGTAATTGGTGGAGGAATTGG
pmt-I136V-rev	TTCCTCCACCAATTACCAAAACCTTTTTTGGATTAGG
pmt-T117Q-fwd	TGGATTTCCATATCAAGAAATGATTGTTCATCTCC
pmt-T117Q-rev	AGATGAACAATCATTTCTTGATATGGAAATCCACC

Rosetta-gami (DE3) cells (Merck Biosciences) for protein expression by standard protocols. Cells were grown in TB Medium with 100 μg/ml ampicillin at 37°C and 250 rpm/min until a density of OD_{600} 0.8–1.0 was reached. IPTG addition, 1 mM for 4–6 h, induced protein expression. Cells were centrifuged (20 min, 4°C, 4500 *g*) and kept on ice for 30 min in lysis buffer containing lysozyme (Sambrook et al. 1989). After sonication, DNase digestion and centrifugation (20 min, 4°C, 11180 *g*) the solution was filtrated (0.45 μm). Enzymes were purified twice through a HiTrap Chelating column on ÄKTA explorer 100 (GE Healthcare Europe) with gradient elution by imidazole (10–500 mM). They were used for activity measurements, when they were approximately 95% pure as estimated from dilution series on SDSP-PAGE and Coomassie staining (not shown). Protein concentration was determined photometrically using bovine serum albumin as standard (Bradford 1976). Expression and purification was controlled by SDS-PAGE (Laemmli 1970) with Coomassie Blue staining.

Enzyme activity

Standard enzyme assays contained ca. 1 μg enzyme, 1 mmol putrescine, 1 mmol SAM or dcSAM in 500 μl glycine–buffer pH 9.0 at 30°C and were stopped with 17 M NaOH. For kinetic measurements of PMT, putrescine and SAM concentrations were varied accordingly. At least two independent protein expressions were used for each data series, each measurement

was repeated at least twice. Enzyme velocity was determined by HPLC measurement (Merck LaChrom) of the dansylated reaction products *N*-methylputrescine or spermidine (Marcé et al. 1995) using fluorimetric detection (365 nm excitation, 510 nm emission) in addition to diode array detection. Each dansylation and HPLC measurement was done in duplicate, so that each data point contained at least eight HPLC measurements. Standard deviations were calculated over all single measurements. PMT activity was measured photometrically by a coupled enzymatic assay based on the conversion of the product SAH to homocysteine by 5′-methylthioadenosine/*S*-adenosylhomocysteine nucleosidase (EC 3.2.2.9) and *S*-ribosylhomocysteine lyase (EC 4.4.1.21). Homocysteine after reaction with 5,5′-dithiobis-2-nitrobenzoic acid yielded a yellow product (Biastoff et al. 2006).

Northern blotting

Plant tissues or root cultures (3 g per sample) were washed quickly with water, blotted dry and frozen in liquid nitrogen. Total RNA was extracted from plant tissues by phenol and chloroform (Sambrook et al. 1989), separated by electrophoresis on 1.2% formaldehyde agarose gel, and blotted onto a Hybond N+ nylon membrane (Amersham-Biosciences). Due to sequence similarity of *pmt* cDNA and *spds* cDNA, probe specificity for *pmt* had to be assured. 5′-terminal fragments for *pmt* (*C. sepium* 175 bp, *D. stramonium* 200 bp, *L. esculentum* 161 bp; primers: Table 1) and a full-length probe for *spds* proved to be sufficiently specific (Fig. 2). Hybridisation with [^{32}P] ATP-labelled DNA probes was done in buffer containing 50% formamide, 5-fold·Denhardt's solution, 1% w/w SDS, 10% w/w dextrane sulphate and 100 µg/ml herring sperm DNA. After blotting the membrane was washed with 2-fold SSC, 0.1% w/w SDS at room temperature for 10 min, once with 1fold SSC, 0.1% w/w SDS at 58°C, and twice with 0.2-fold SSC, 0.1% w/w at 58°C for 20 min. Equal loading was confirmed by re-hybridisation of the membrane with a 18S rRNA probe from *L. esculentum.*

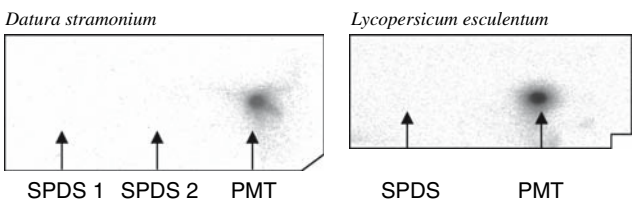

Fig. 2 Dot blot for control of *pmt* probe specificity with 1 µg plasmid DNA per spot. PMT partial sequence probes were labelled by ^{32}P-ATP

RT-RCR

RNA preparations used for Northern blotting were transcribed into cDNA using the plant-specific primers for the full-length clones of *pmt* and *spds* for control. For *C. sepium*, a *β*-amylase fragment (primers: Table 1) was used as positive control instead of *spds*. PCR products were separated in a agarose gel and stained by ethidium bromide.

Mutagenesis

Primer for mutagenesis were designed of a minimum length of 30 bp with the desired mutation in the middle and a melting temp. of 60–70°C. For control, a silent mutation was introduced in addition to the desired amino acid exchange when possible to provide an additional restriction site. Plasmide construction and PCR amplification was done according to the QuikChange II Site-Directed Mutagenesis Kit (Stratagene) with reduction of the reaction volume to 25 µl.

Modelling and substrate docking

Proteins homologous to PMT with a resolved X-ray structure and at least 30% identity were identified by BLASTP search (Altschul et al. 1990) in the Swiss-Prot database. Spermidine synthase I from *Arabidopsis thaliana* (cc no Q9ZUB3, pdb-code 1XJ5, gene at1g23820) appeared most similar. Except for the first 52 residues of SPDS, for which no significant alignment with DsPMT could be obtained, a homology of 69.1% (e-value e^{-108}) resulted, which is sufficient for homology modelling. Using the molecular modelling program MOE (molecular operating environment, Chem. Comp. Group. Inc., Montreal, Canada) the sequence of Ds-PMT was aligned to that of 1XJ5 with the BLOSOM70-substitution matrix (Henikoff and Henikoff 1992, 1993). Ten structures of Ds-PMT were generated and structure energy was minimized using Charmm22 (MacKerell et al. 1998) and Born-Solvation (Pellegrini and Field 2002). All structures were checked for stereochemical quality with PROCHECK (Laskowski et al. 1993) and for native folding with PROSA II (Sippl 1990). Some outliers appearing in the disallowed region of the Ramachandran plot were either manually modified or could be moved to allowed regions by short molecular dynamics simulations (10 ps, 500 K) and subsequent minimization. Thereafter, parameters for good stereochemical quality of the structures were fulfilled, 84.6% aa in most favoured region, 15.4% in additionally allowed regions (by PROCHECK). PROSA analysis showed all residues, except for the

first 20 residues, in the negative energy area and with a combined energy *z*-score of –9.38, which is in the expected range for a protein with 292 modelled aa and a native fold. The docking of SAM was achieved by superposition of the backbone structures of the model and of the X-ray structure, followed by merging the cosubstrate to the model and subsequent energy optimization. The substrate putrescine was docked to the active site using the automatic docking program GOLD (Genetic Optimized Ligand Docking, Cambridge Crystallographic Data Centre, 1998, Cambridge, UK) (Jones et al. 1995, 1997; Nissink et al. 2002; Verdonk et al. 2003) with standard values given by the program. From the resulting 30 docking arrangements the one with expected orientation of one amino group close to the active methyl group of SAM was used for further energy refinement to capture slight induced fit modifications of the proteins active site as all amino acid residues of the protein are fixed during the docking procedure.

Results

PMT cloning and expression

Primers for *pmt* were designed with the aim to obtain large PCR fragments that enabled distinction between *pmt* and *spds* before RACE-completion of the sequence, protein expression, and determination of catalytic activity. PCR yielded two fragments from *D. innoxia* of 662 bp and 665 bp length that were more similar to *pmt* than to *spds*, and one equivalent fragment of 662 bp from *D. stramonium*. Completion of the full coding sequence and protein expression in *E. coli* confirmed that all three enzymes possessed PMT activity. The same primer combinations were applied to root cDNA of *Physalis divaricata*, Solanaceae, and PCR yielded a *pmt*-like fragment of 662 bp length. Phytochemical investigation of *P. divaricata* root cultures accordingly revealed calystegines (Table 2) and other tropane alkaloids. A similar *pmt*-like fragment (650 bp) was amplified from tomato root mRNA, and calystegines were identified in tomato roots, stems, and leaves in addition to fruits (Table 2). PCR on root culture cDNA of *Solanum dulcamara* yielded a *pmt*-like fragment (650 bp). Finally, the PCR search was extended to mRNA from root cultures of *Calystegia sepium*, Convolvulaceae, that form calystegines (Scholl et al. 2001). Again, two 659 bp long *pmt*-like fragments were obtained. All PCR-fragments were completed to full reading frames by RACE-PCR, except the second *C. sepium* fragment, which was recalcitrant to 5′-RACE. The sequence lacked about 120 bp at the 5′-end. As *pmt* sequences vary in the 5′ region, a start codon ATG was introduced by PCR into the shortened sequence (Table 1, primer Cs-*pmt2*-fwd-*Nco*I). After translation into amino acids, all sequences showed identity values between 76% and 97% by Clustal W 1.83 among each other and comparable similarities to other published PMT sequences. Similarity to Solanaceae SPDS was somewhat lower, between 58% and 68% (Fig. 3). CsPMT2, the abbreviated PMT, appears to be more similar to other PMTs than CsPMT1, but all PMTs show highest variability in the N-terminus, which is missing in CsPMT2, thus the identity of the remaining parts is higher (gaps were ignored for homology scores). When only the central parts (aa 40–340) of all PMTs were compared, identity ranged between 82% and 95%, still CsPMT1 showing the lower values. The finding of two sometimes divergent *pmt* sequences in several plants was pursued by Southern blotting. Full-length *pmt*-probes detected three to four DNA-fragments that were generated by enzymes not recognising a restriction site within the coding sequence. Southern blot results (not shown) together with PCR amplification indicate more than one non-allelic *pmt* gene in each genome. All proteins were expressed in *E. coli* and purified. PMT catalytic activity was confirmed for all enzymes and was exclusive; incubations with putrescine and dcSAM did not produce spermidine. Maximal activity was measured at pH 9.0 and ranged between 1.2 and 10 nkat per mg protein corresponding to turnover numbers of 0.05–0.39 per second (Table 3). K_M values for putrescine on all PMTs above 100 μM appeared higher than K_M of putrescine on SPDS, which are typically between 12 μM and 36 μM.

Transcripts of *pmt* were localised in plants and root cultures by Northern blotting. Only roots and root cultures showed *pmt* transcripts for *D. stramonium, L. esculentum*, and *C. sepium* (Fig. 4). Northern blotting may lack sensitivity due to limited probe labelling or hybridisation, therefore RT-PCR amplification of *pmt* transcripts from roots and aerial plant tissues was performed in addition. Spermidine synthase cDNA representing a ubiquitous transcript was amplified as positive control for *D. stramonium* and *L. esculentum*, and a *β*-amylase cDNA fragment for *C. sepium*, as no spermidine synthase sequence was available. Again *pmt* cDNA was amplified from root tissues only (Fig. 5**)**. Sensitivity of PCR amplification was confirmed by *L. esculentum* root cultures that appeared negative on Northern blots but showed *pmt* sequence amplification by PCR.

Table 2 Calystegines and hyoscyamine (μg/gram dry mass) in plants used for *pmt* cloning

	μg/g dm	Cal. A_3	Cal. A_5	Cal. B_1	Cal. B_2	Hyoscyamine
C. sepium	Root	809	–	–	418	–
	Root culture	630	–	300	520	–
D. innoxia	Root culture	1120	–	–	–	4690
D. stramonium	Root	3	–	–	13	2870
	Root culture	6	–	–	7	1020
L. esculentum	Root	3.4	0.9	–	0.8	–
	Root culture	4	1	–	2	–
	Stem	0.4	5	–	0.4	–
	Leaf	0.2	7	–	1.2	–
	Fruit	21	–	–	21	–
P. divaricata	Root culture	7	4.4	8.5	14.7	–

– not detected

PMT motifs and sequence conservation

Alignments of PMT sequences with those of SPDS were performed with the aim to find SAM binding regions and typical distinctions between PMTs and corresponding plant SPDSs that bind dcSAM (Fig. 6). The first α-helix region (aa 111–121; numbering here and in all subsequent comparisons according to Ds-PMT) contains a conserved Thr117. The corresponding Gln or His in SPDS was inferred as responsible for putrescine positioning judging from crystal structure resolution of SPDS from *Theromotoga maritima* and from *Caenorhabditis elegans* (Korolev et al. 2002; Dufe et al. 2005). Seven of the surrounding amino acids (motif 1 in Fig. 6) differ continuously between PMT and SPDS and may serve for distinction of unknown PCR cloning products. Motif 2 for PMTs (aa 136–147) is identical with Prosite signature PS01330 [VAI]-[LAV]-[LIV](2)-G-G-G-x-[GC]-x(2)-[LIVA]-x-E, which is annotated for identification of SPDS and includes PMT. Three of the Gly residues in motif 2 participate in dcSAM binding (Korolev et al. 2002). Six of the 12 amino acids of the signature differ between PMT and SPDS, among them Ile141 that is exchanged into Asp in all SPDS sequences. Motif 3 comprises a conserved region in helix αC (aa 168–181), in which 10 of 14 amino acids differ between SPDS and PMT. Motif 3 again serves for distinction of PMT sequences. Motif 4 according to the protein model (see below) represents a loop region between β10 and αE (aa 211–222) that is equally conserved (10 of 12 aa) for both, PMT and SPDS. D211 corresponds to the catalytic aspartate to which substrate deprotonation in the active centre is attributed in SPDS. All four motifs were tested by FASTA search. Motif 1 and 2 retrieved PMT sequences only; SPDS was retrieved in addition to PMT with motifs 3 and 4, but with clearly less similarity.

From the crystal structure of SPDS in complex with the inhibitor *S*-adenosyl-1,8-diamino-3-thiooctane (AdoDATO) 20 amino acids were identified that are in contact with the ligand; they are located in the active site (Korolev et al. 2002). Only two of them discriminate PMT and plant SPDS; they were selected for mutagenesis (highlighted in Fig. 6). T117 corresponds to H77 of *T. maritima* SPDS that binds to the aminoethyl residue of AdoDATO and is inferred to bind the aminopropyl part of dcSAM. T117 was mutated to Q, the corresponding amino acid in plant SPDS. I141 of Ds-PMT was exchanged for D, which is assumed to prevent SAM binding in SPDS (D101 in the *T. maritima* enzyme) by occupying the space for the carboxyl group of SAM. In the same motif, I136 was changed to V to test whether a small change in the vicinity but not within the active centre would make a difference in catalysis. Finally a cumulative exchange of T117Q and I141D should reveal, whether SPDS activity can easily be generated in the PMT protein frame. Mutated proteins DsPMT-T117Q and DsPMT-I141D were expressed as soluble proteins, but displayed neither PMT nor SPDS activity. The same was observed for the double mutant DsPMT-T117Q+I141D. Mutation DsPMT-I136V after expression showed reduced PMT activity of 5216 pkat per mg protein (standard deviation 319, $n = 3$), which corresponds to about half of the wild type DsPMT activity. The strikingly strong effect of each single mutation initiated modelling of the PMT polypeptide structure.

The model of DsPMT with the cosubstrate SAM and the substrate putrescine docked in the active site yielded a structure similar to the protein fold and structure of spermidine synthase from *Thermotoga maritima* (TmSPDS) with AdoDATO as ligand (Korolev et al. 2002) (Fig. 7**).** Both structures share the glutamate (E161 DsPMT, E121 TmSPDS) responsible for the recognition of the adenosin sugar moiety. The conserved D211 (D170 TmSPDS) very likely participates in the catalysis or at least in the recognition of the positively charged sulphur in SAM. In the first step of docking SAM to the model of PMT, SAM orientation was copied from that of the assumed dcSAM in

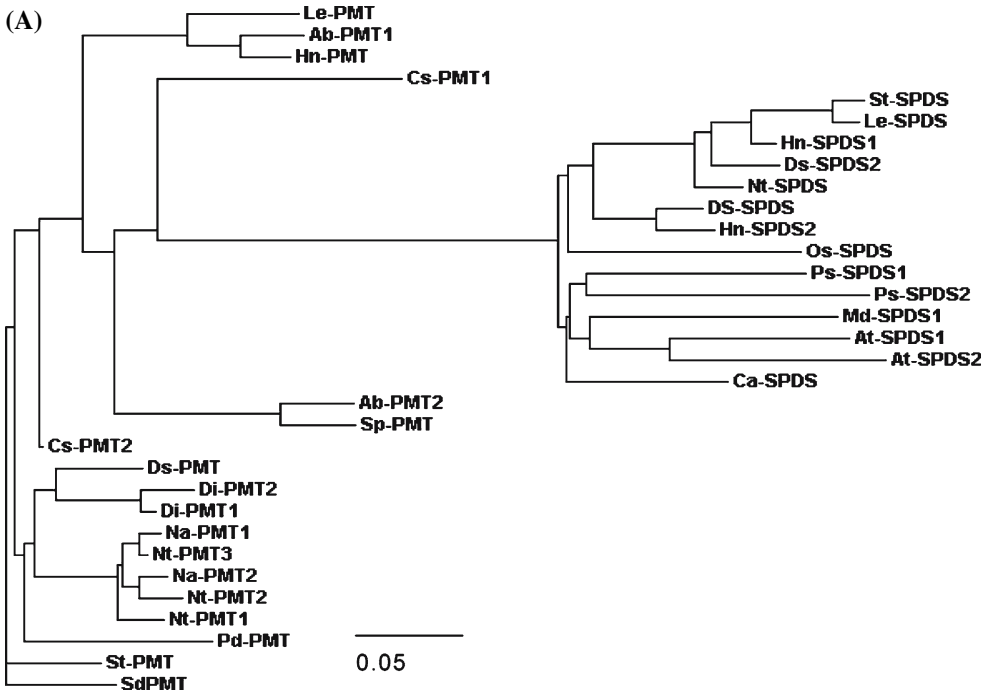

Fig. 3 (**A**) Phylogenetic tree and (**B**) identity comparison of PMT and SPDS by Clustal W 1.83. The unrooted tree was constructed by the neighbour joining method. PMT and SPDS sequences were from *Calystegia sepium* (Cs), *Datura innoxia* (Di), *Datura stramonium* (Ds), *Lycopersicum esculentum* (Le), *Physalis divaricata* (Pd), *Solanum dulcamara* (Sd), *Atropa belladonna* (Ab), *Hyoscyamus niger* (Hn), *Nicotiana attenuata* (Na), *N. tabacum* (Nt), *Solanum tuberosum* (St), *Arabidopsis thaliana* (At), *Coffea arabica* (Ca), *Malus domestica* (Md), *Oryza sativa* (Os), Pisum sativum (Ps)

(B)

	aa	Cs PMT1	Di PMT1	Ds PMT	Le PMT	Pd PMT	Sd PMT	EMBL accession
CsPMT1	344	100	77	78	77	76	80	AM177608
CsPMT2	302	85	92	92	89	91	95	----
DiPMT1	340		100	92	82	86	91	AM177609
DiPMT2	341		97	90	82	85	90	AM177610
DsPMT	344			100	82	88	90	AJ583514
LePMT	340				100	80	81	AM177607
PdPMT	342					100	86	AM177611
SdPMT	340						100	----
AbPMT1	336	78	90	84	91	81	81	AB018570
AbPMT2	340	77	80	80	78	79	80	AB018571
HnPMT	338	77	83	81	90	78	85	AB018572
NaPMT1	388	79	90	90	84	85	88	AF280402
NaPMT2	371	78	90	90	84	85	89	AF280403
NtPMT1	375	80	90	90	84	87	89	AF126810
NtPMT2	353	78	89	89	83	85	86	AF126809
NtPMT3	381	80	90	90	84	86	91	AF126811
SpPMT	359	80	81	82	80	81	82	AY762993
StPMT	340	80	88	90	81	87	91	AJ605553
AtSPDS1	334	64	61	60	61	60	60	AJ251296
AtSPDS2	340	61	59	60	58	58	59	AJ251297
Ca SPDS	316	66	66	66	66	66	65	AB015599
DsSPDS1	308	68	67	67	67	66	68	Y08252
DsSPDS2	317	66	64	64	63	63	64	Y08253
HnSPDS1	315	65	64	64	65	63	64	AB006690
HnSPDS2	308	67	67	67	66	66	67	AB006691
LeSPDS	342	61	59	59	59	58	60	AJ006414
MdSPDS1	335	62	61	62	61	60	60	AB072915
NtSPDS	261	68	65	65	66	65	65	AF321139
OsSPDS	323	65	63	63	63	62	63	AJ251298
PsSPDS1	334	63	60	63	61	60	61	AF043108
PsSPDS2	342	61	66	59	59	61	61	AF043109
StSPDS	347	61	60	58	59	59	60	AJ345003

Table 3 Kinetic properties of PMTs, two plant SPDS for comparison

	K_M putrescine (μM)	V_{Max} (pkat/mg protein)	Kcat (1/s)	References
Calystegia sepium PMT1	120	4118	0.160	This study
Calystegia sepium PMT2	–	2500	0.086	
Datura stramonium	281	10030	0.388	
Lycopersicum esculentum	113	4943	0.190	
Datura innoxia PMT1	–	10000	0.383	
Datrura innoxia PMT2	–	9340	0.359	
Physalis divaricata	–	5128	0.198	
Solanum dulcamara	169*	1200	0.047	
*Datura stramonium***	310	7386		Walton et al. (1994)
*Hyoscyamus albus***	277	385		Hibi et al. (1992)
Solanum tuberosum	242	3430	0.131	Stenzel et al. (2006)
*Glycine max*** (SPDS)	33	1278		Yoon et al. (2000)
Solanum tuberosum (SPDS)	–	3096	0.121	Stenzel et al. (2006)

K_M and V_{Max} averaged from 3 independent determinations, sd < 5%

Kcat was calculated for enzyme preparations obtained by heterologous expression that appeared homogenous after purification

*Data obtained by photometric assay

**Enzymes purified from plant tissue

– not determined

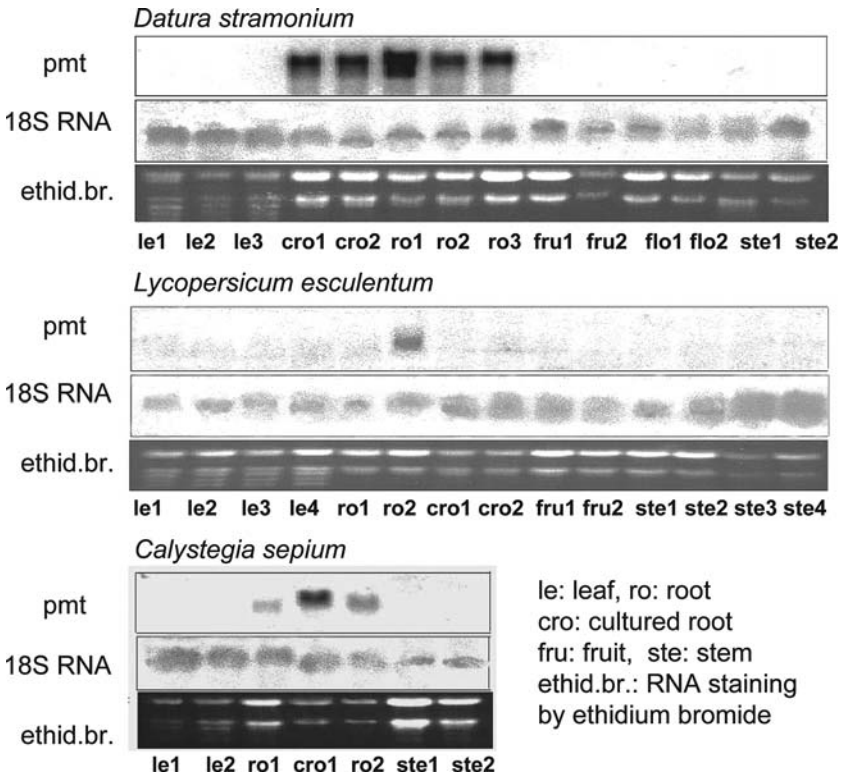

Fig. 4 Northern blots of *D. stramonium, L. esculentum*, and *C. sepium* RNA obtained from various plant organs. Specific probes for *pmt* transcripts (Fig. 2) were hybridised to RNA fixed to the membrane (upper panel) followed by hybridsation with a 18S rRNA probe from *L. esculentum* for RNA quality control (middle panel). RNA loading was controlled by ethidium bromide (ethid.br.) staining (lower panel)

TmSPDS. However, only the adenosyl moiety could be placed in a spatial and electronic favourable position into the binding pocked of PMT. In SPDS the protonated ethylamino group of AdoDATO forms a salt bridge to D101 (Fig. 7B). Due to the exchange of the corresponding residue by isoleucine in PMT, such an arrangement of the protonated N-terminus of SAM is impossible. To identify an appropriate position of the amino acid part of SAM the group was rotated to several alternate conformations, which were subsequently minimized allowing induced fit of the side chains of amino acids of the protein. This docking of SAM to PMT is stabilized by hydrogen bonds formed between the protonated N-terminus and the side chain of Q107 and of the carboxyl group forming a hydrogen bond to Q244 (Fig. 7A). The local pKa-values of ionic

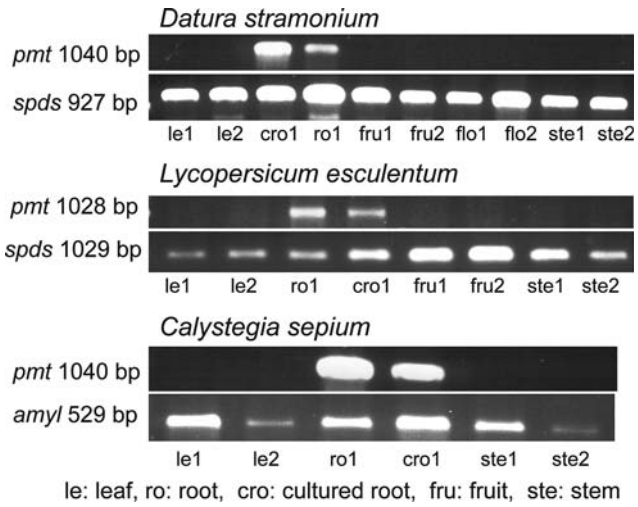

Fig. 5 PCR of *pmt* cDNA from *D. stramonium*, *L. esculentum*, and *C. sepium* mRNA obtained from various plant organs (upper panel). Control PCR (lower panel): *spds* full-length spermidine synthase cDNA; *amyl*: fragment of *C. sepium* β-amylase cDNA

amino acid residues surrounding the ligands were determined using the option in MOE based on a recently published function for prediction (Li et al. 2006) assuming an overall pH of 7.0. E110 in the active site is supposed to recognize putrescine and the pKa-value was predicted to be 2.00. For E161, which forms two hydrogen bonds with sugar moiety of SAM, the pKa-value was assigned to 4.65, and for the assumed catalytic D211 close to the sulphur atom of SAM it was 4.26. These residues will be deprotonated at neutral pH. The local pKa-value of the putrescine nitrogen atom forming the salt bridge to E110 was predicted as 10.1, the other nitrogen had a pKa of 7.64. According to these predictions, one putrescine nitrogen will bind in the protonated form to the E110 anion, whereas the other nitrogen is close to the equilibrium between protonation and non-protonation, slightly favoured to be protonated at pH 7.0, however deprotonated at higher pH. Maximal activity of PMT is measured at pH values above 8, where the second putrescine nitrogen is rather deprotonated and more accessible to methyl transfer. Long range electrostatic interactions (~5 Å) of the positively charged protonated N-terminus of SAM with the negatively charged side chain of D214 will stabilise the arrangement of SAM in the active site. The corresponding D173 in TmSPDS interacts with the amino group of AdoDATO in the putrescine-mimicking position. The equivalent position for the substrate putrescine in the SPDS fold is with the docking of SAM to PMT now occupied by the amino acid part of SAM. Putrescine is not able to dock from this side. The only accessible space demands a slight change in the side chain conformation of E110 (in comparison to E70 in TmSPDS) and leads to the recognition of one protonated nitrogen of putrescine. The other reactive amino group forms hydrogen bonds to D211 and H108.

Discussion

PMT kinetics and localisation

After selection of appropriate primers for the straightforward cloning of PMT sequences, the expression of enzyme proteins for characterisation of the individual catalytic properties was readily achieved. The velocity of methyl transfer catalysed by the PMTs appeared in the same order of magnitude and comparable to SPDS as well as to other heterologously expressed plant *N*-methyltransferases (Smith et al. 2000; Choi et al. 2002). Kinetic measurements of PMTs are laborious due to the HPLC evaluation that demands derivatisation, frequent assay repetitions, and extensive calibration. A photometric assay for methyltransferases replacing HPLC measurements was developed in the course of this study (Biastoff et al. 2006), but assays here were analysed by HPLC for comparability to former results. When SAH was directly metabolised by adenosylhomocysteine nucleosidase in the photometric assay, maximal activity V_{Max} for PMT appeared higher, e.g., 39 nkat/mg protein for *D. stramonium* PMT and 3.5 nkat/mg protein for *S. dulcamara* PMT. The reason is attributed to product inhibition by SAH in in vitro assays that was reported often for methyltransferases (Moffatt and Weretilnyk 2001). Affinity for putrescine on PMT expressed as K_M was low when measured by HPLC, however, product inhibition by SAH will also influence K_M assuming an ordered bi-bi-mechanism (Hibi et al. 1992). By addition of SAH degrading enzyme, K_M for putrescine decreased, yet, the affinity of putrescine to PMT remained lower than to SPDS (Biastoff et al. 2006). It may be hypothesised that by differential affinity plant cells expressing PMT are protected against excessive drains of the essential diamine putrescine into alkaloids metabolism. On the other hand, PMT enzymes, despite of rather inefficient putrescine binding in vitro, may function in a channelled multienzyme complex, in which SAH is directly destroyed. Evidence for a complex of diamine oxidase and SAH hydrolase was shown for nicotine biosynthesis (Heim and Jelesko 2004).

Putrescine *N*-methyltransferase protein expression was reported to be confined to roots in nicotine (Zhang and Baldwin 1997; Shoji et al. 2000) and tropane alkaloid producing plants (Suzuki et al. 1999), the only

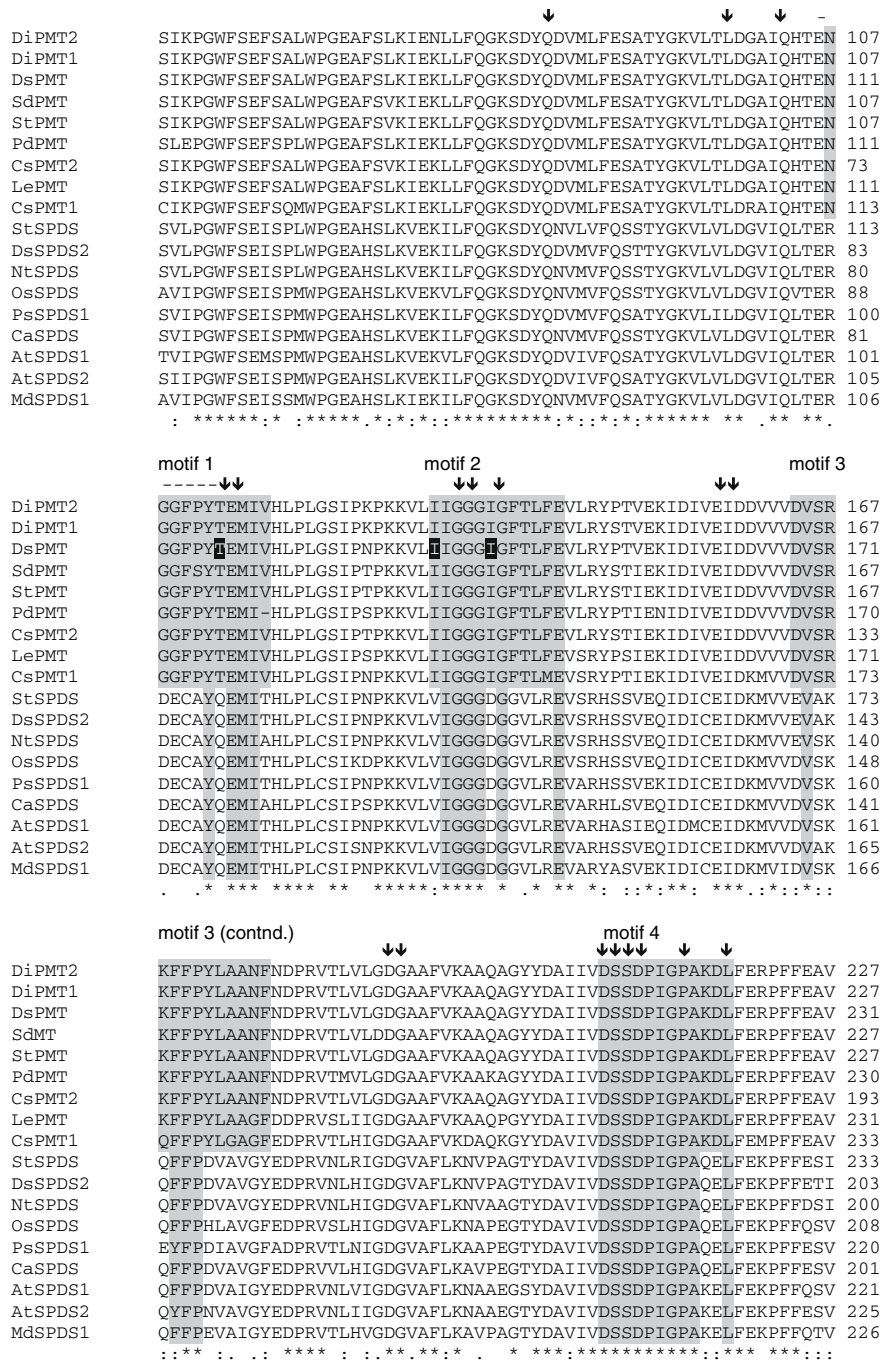

Fig. 6 Partial sequence alignment by Clustal W 1.83. Symbols above the sequences: ↓ = Substrate and cosubstrate binding sites (Korolev et al. 2002); - - - - Primer binding site in cDNA. Symbols below the sequences: * identical amino acids; **:** similar amino acids; **.** different amino acids. Abbreviations for sequences are identical to Fig. 3. Amino acids shaded in grey: 4 motifs. Amino acids white on black background: aa for mutagenesis. T117 in motif 1 (numbering of DsPMT) corresponding to Q in SPDS was mutated to Q, because it is assumed to be responsible for putrescine positioning in SPDS; 7 surrounding aa of motif 1 differ between PMT and SPDS. Motif 2 is identical with Prosite signature PS01330 for SPDS and includes PMT; 6 of 12 aa of the signature differ between PMT and SPDS, among them I136 and I141. They were mutated into V and D, respectively. Motif 3 comprises a PMT conserved region with 10 of 14 aa differing from SPDS and serving for distinction of PMT and SPDS. Motif 4 is conserved (10 of 12 aa) for both, PMT and SPDS. It contains D211, catalytic aspartate, to which substrate deprotonation in the active centre is attributed in SPDS

```
                                                                    ↓    ↓
DiPMT2        AKALRPGGVVCTQAESIWLHMHIIKQIIANCRQVFKGSVNYAWTTVPTYPTGVIGYMLCS 287
DiPMT1        AKALRPGGVVCTQAESIWLHMHIIKQIIANCRQVFKGSVNYAWTTVPTYPTGVIGYMLCS 287
DsPMT         AKALRPGGVVCTQAESIWLHMHIIKQIIANCRQVFKGSVNYAWTTVPTYPTGVIGYMLCS 291
SdPMT         AKALRPGGVVCTQAESIWLHMHIIKQIIANCRQVFKGSVNYAWTTVPTYPTGVIGYMLCS 287
StPMT         AKALRPGGVICTQAESIWLHMHIIKQIIANCRLVFKGSVNYAWTTVPTYPTGVIGYMLCS 287
PdPMT         AKALRPGG-VCTQAESIWLHMHIIKQIIANCRQVFKGSVNYAWTTVPTYPTGVIGYMLCS 289
CsPMT2        AKALRPGGVVCTQAESIWLHMHLIKQIIANCRQVFKGSVNYAWTTVPTYPTGVIGYMLCS 253
LePMT         AKALRPGGVVCTQAESIWLHMHLIKKIIANCRQVFKGSVNYAWTTVPTYPTGVIGYMLCS 291
CsPMT1        AKALRPGGVVCTQAESIWLHMHFIKQIIASCRQVFKGSVNYAWTTVPTYPSGVIGYMLCS 293
StSPDS        AKALRPGGVVATQAESIWLHMHIIEEIVANCRQIFKGSVNYAWTTVPTYPSGMIGFMLCS 293
DsSPDS2       ARALRPGGVVSTQAESIWLHMHIIEEIVANCREIFKGSVNYAWTTVPTYPSGMIGFMLCS 263
NtSPDS        ARALHPGGVVSTQAESIWLHMHIIEEIVANCRQIFKGSVNYAWTTVPTYPSGMIGFMLCS 260
OsSPDS        ARALRPGGVVCTQAESIWLHMHIIEDIVANCRQVFKGSVNYAWTTVPTYPSGVIGFMLCS 268
PsSPDS1       ARALRPGGVVCTQAESIWLHMHIIEDIVVNCRQVFKGSVNYAWTTVPTYPSGMIGFMLCS 280
CaSPDS        AKALRPGGVVCTQAESIWLHMHIIEDIVANCRQIFKGSVNYAWTTVPTYPSGVIGFMLCS 261
AtSPDS1       ARALRPGGVVCTQAESLWLHMDIIEDIVSNCREIFKGSVNYAWTSVPTYPSGVIGFMLCS 281
AtSPDS2       NRALRPGGVVCTQAESLWLHMDIIEDIVSNCRDIFKGSVNYAWTSVPTYPSGVIGFMLCS 285
MdSPDS1       ANALRPGGVVCTQAESIWLHMHIIEDIVANCREIFKGSVNYAWTTVPTYPSGVIGFMLCS 286
               .**:***::.*****:****.:*:.*: .** :**********:*****:*:**:****

                                                 --------
DiPMT2        TEGPEVDFKNPVNAIDKLDETHVNSKLGPLKFYNTDIHKSAFILPSFAKNLTES--- 341
DiPMT1        TEGPEVDFKNPVNPIDK-DETHANSKLGPLKFYNTDIHKAAFILPSFARSMIES--- 340
DsPMT         TEGPEVDFKNPVNPIDK-DETHANSKLGPLKFYNTDIHKAAFILPSFARSMIES--- 344
SdPMT         TEGPEVDFKNPINPIDK-DSTHVKSKLGPLKFYNSDIHKAAFILPSFARSLIES--- 340
StPMT         TEGPEVDFKNPVNPIDK-DTTHVKSKLEPLKFYNTDIHKAAFILPSFARSLIES--- 340
PdPMT         TEGPEVDFKNPVNPIDK-ATAHIKSELGPLKFYNSDIHKAAFILPSFAASLIES--- 342
CsPMT2        TEGPEVNFKNPVNSIDK-DTTHVKSK-GPLKFYNSDIHK-AFTLPSFVQKLL----- 302
LePMT         TEGPEVNFKNPVNSIDK----YVKSK-GPLKFYNSDIHKSAFILPSFARDLFES--- 340
CsPMT1        TEGPDVDFKNPVNPIDK-DTSHVKSK-GPLKFYNAEIHKAAFTLPSFVQKLLE---- 344
StSPDS        TEGPAVDFKNPINPIDD---ESPVKTIEPLKFYNSEIHQASFCLPSFAKRVIETKGK 347
DsSPDS2       TEGPAVDFKNPINPIDD---ESHGQTIGPLKFYNSEIHQASFCLPSFAKRVIETKGK 317
NtSPDS        T---------------------------------------------------------- 261
OsSPDS        TEGPTVDFQHPIFNIED--NEFSTKSKGPLKFYNSEIHSASFCLPSFAKRVIGSKAN 323
PsSPDS1       TEGPSVDFKHPVNPIDE--NDSQ-QAARPLKFYNREIHSAAFCLPSFAKRAIASKEN 334
CaSPDS        TEGPPVDFKHPINPIDA--NDGRSKTMKPLKFYNSEIHSAAFCLPSFAKKVIDSKAN 316
AtSPDS1       TEGPDVDFKHPLNPID----ESSSKSNGPLKFYNAEIHSAAFCLPSFAKKVIESKAN 334
AtSPDS2       SEGPQVDFKKPVSLIDT--DESSIKSHCPLKYYNAEIHSAAFCLPSFAKKVIDSKAN 340
MdSPDS1       TEGTAVDFKHPVNSID--------ESKRPLRFYNSEIHTAAFCLPSFAKKVIDAKAK 335
               :    : :   :  :              :      :    : :  :
```

Fig. 6 continued

exceptions being young potato tuber sprouts that synthesise calystegines (Stenzel et al. 2006) and wounded leaves of tobacco (Sachan and Falcone 2002). Exclusive *pmt* transcript localisation in roots was confirmed for all plants included in this study and should be considered as typical for non-wounded plants. Transport of calystegines or preceding metabolites into aerial organs must be inferred from the expression of PMT usually restricted to roots.

Motifs and mutations

The PMT sequences including PMT from Convolvulaceae demonstrate that the natural variation of these sequences is limited. Large segments of the PMTs appear conserved. Similarities, however, to other methyltransferases including plant small molecule *N*-methyltransferases stay below 10% as indicated before (Stenzel et al. 2006). Determination of the three-dimensional structures of plant *O*-methyltransferases confirmed a structural conservation for the glycine-rich SAM binding motif (Zubieta et al. 2001). This motif is found in PMTs as motif 2. PMTs due to their descent from SPDS have little more in common with other methyltransferases. SPDS is assumed as distinct from methyltransferases already in LUCA, the last universal common ancestor cell (Kozbial and Mushegian 2005). Compared to SPDS, PMT sequences displayed four consensus motifs typically different from SPDS, which simplifies PMT identification in primary sequences. Tandem repeats at the N-terminus of PMTs, however, were not found and appear to be restricted to PMT sequences from *Nicotiana* species. For the search of calystegines, PMT conservation offers a practical advantage. Calystegine occurrence in plants is tedious to analyse due to hydrophilic behaviour and lack of chromophor. Efficient and specific PMT transcript amplification as cDNA may serve as indicator for the presence of the tropane alkaloid pathway. Calystegines were reported from Brassicaceae recently, and it will be interesting to investigate sequences and the characteristics of an implied PMT activity in Brassicaceae.

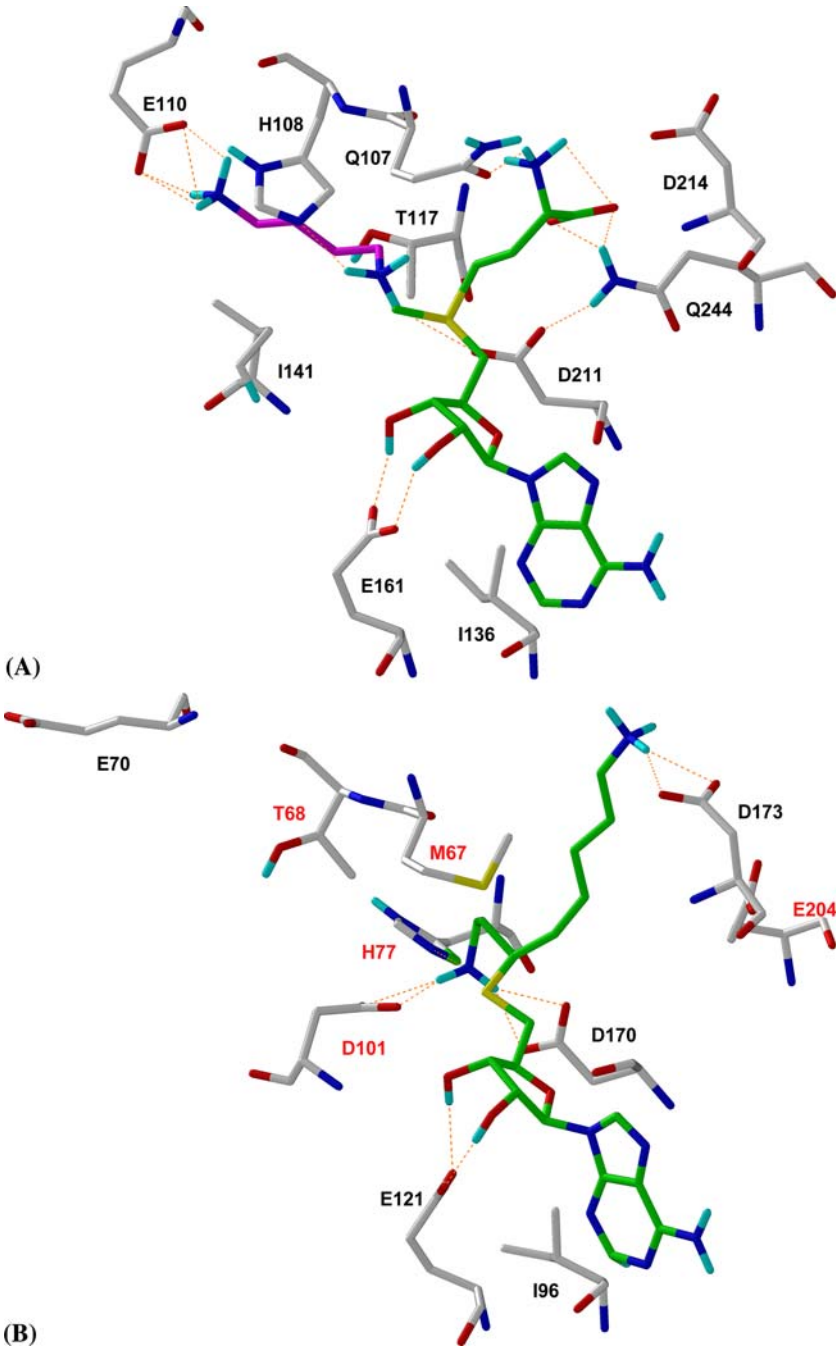

Fig. 7 (**A**) Active site of the model of Ds-PMT with SAM (green) and putrescine (magenta) (**B**) Active site obtained from the crystal structure of *T. maritima* SPDS with the inhibitor *S*-adenosyl-1,8-diamino-3-thiooctane. Amino acid residues labelled in red are different between both structures. Dotted orange lines signify hydrogen bonds or salt bridges

Mutagenesis was attempted on the basis of the aligned PMT and SPDS sequences. Complete loss of function was observed when two amino acids were exchanged that were assumed to be in contact with the cosubstrate. An exchange of isoleucine to valine adjacent to the assumed active site of PMT reduced activity to half. Modelling of PMT suggested that SAM must adopt a position in the enzyme's active site different from the equivalent placement of dcSAM in SPDS concluded from AdoDATO co-crystallisation. Thus, the amino acids of PMT chosen for mutagenesis possess different function than inferred from the SPDS structure. The DsPMT-T117Q and DsPMT-I141D mutants appear to cause an aberrant positioning of putrescine that disables methyl transfer. Considering the position of DsPMT-I137 the exchange I136V may have caused a slightly different binding of SAM with the consequence of impaired but not complete loss of catalysis. The results point out that PMT alignments to the structurally established SPDS proteins can be misleading, when substrate or cosubstrate binding sites are inferred. PMT has probably developed a slightly altered protein

scaffold and differences in the active site when evolving from SPDS. In consequence, sequence alignment and protein modelling without structure resolution from crystallisation are insufficient for assigning functions and positions of amino acids in PMT.

Acknowledgement Professor Keiji Samejima, Josai University, Saitama, Japan, kindly donated dcSAM. The Botanic Garden of Martin Luther University kindly provided and authenticated seed material. Helpful discussions and correction of the manuscript by Dr. Y. Sichhart and S. Biastoff and technical assistance by S. Brauer, C. Harnisch, and B. Schöne in the Institute of Pharmacy are highly appreciated. M.E.A. and F.N. gratefully acknowledge PhD scholarships by the Ministry of Health and Medical Education of the Islamic Republic of Iran. Studies in the Institute of Pharmacy and at the Leibniz Institute of Plant Biochemistry were financially supported by the German research foundation (DFG).

References

Altschul SF, Gish W, Miller W, Myers EW, Lipman DJ (1990) Basic local alignment search tool. J Mol Biol 215:403–410

Asano N, Kato A, Matsui K, Watson AA, Nash RJ, Molyneux RJ, Hackett L, Topping J, Winchester B (1997) The effects of calystegines isolated from edible fruits and vegetables on mammalian liver glycosidases. Glycobiology 7:1085–1088

Asano N, Kato A, Oseki K, Kizu H, Matsui K (1995) Calystegins of *Physalis alkekengi* var. *francheti* (Solanaceae). Structure determination and their glycosidase inhibitory activities. Eur J Biochem 229:369–376

Asano N, Oseki K, Tomioka E, Kizu H, Matsui K (1994a) N-containing sugars from *Morus alba* and their glycosidase inhibitory activities. Carbohydr Res 259:243–255

Asano N, Tomioka E, Kizu H, Matsui K (1994b) Sugars with nitrogen in the ring isolated from the leaves of *Morus bombycis*. Carbohydr Res 253:235–245

Beresford PJ, Woolley JG (1974) Biosynthesis of Tigloidine in *Physalis peruviana*. Phytochemistry 13:2143–2144

Biastoff S, Teuber M, Zhou ZS, Dräger B (2006) Colorimetric activity measurement of a recombinant putrescine *N*-methyltransferase from *Datura stramonium*. Planta Med 72:1136–1141

Bradford MM (1976) A rapid and sensitive method for the quantitation of microgram quantities of protein utilizing the principle of protein–dye binding. Analyt Biochem 72:248–254

Brock A, Herzfeld T, Paschke T, Koch M, Draeger B (2006) Brassicaceae contain nortropane alkaloids. Phytochemistry 67:2050–2057

Choi KB, Morishige T, Shitan N, Yazaki K, Sato F (2002) Molecular cloning and characterization of coclaurine *N*-methyltransferase from cultured cells of *Coptis japonica*. J Biol Chem 277:830–835

Dufe VD, Lüersen K, Eschbach M-L, Haider N, Karlberg T, Walter RD, Al-Karadaghi S (2005) Cloning, expression, characterisation and three-dimensional structure determination of *Caenorhabditis elegans* spermidine synthase. FEBS Lett 579:6037–6043

Gamborg OL, Miller RA, Ojima K (1968) Nutrient requirements of suspension cultures of soybean root cells. Exp Cell Res 50:151–158

Griffin WJ, Lin GD (2000) Chemotaxonomy and geographical distribution of tropane alkaloids. Phytochemistry 53:623–637

Hashimoto T, Tamaki K, Suzuki K, Yamada Y (1998a) Molecular cloning of plant spermidine synthases. Plant Cell Physiol 39:73–79

Hashimoto T, Shoji T, Mihara T, Oguri H, Tamaki K, Suzuki K-I, Yamada Y (1998b) Intraspecific variability of the tandem repeats in *Nicotiana* putrescine *N*-methyltransferases. Plant Mol Biol 37:25–37

Heim WG, Jelesko JG (2004) Association of diamine oxidase and *S*-adenosylhomocysteine hydrolase in *Nicotiana tabacum* extracts. Plant Mol Biol 56:299–308

Henikoff S, Henikoff JG (1992) Amino acid substitution matrices from protein blocks. Proc Nat Acad Sci USA 89:10915–10919

Henikoff S, Henikoff JG (1993) Performance evaluation of amino acid substitution matrices. Proteins 17:49–61

Hibi N, Fujita T, Hatano M, Hashimoto T, Yamada Y (1992) Putrescine *N*-methyltransferase in cultured roots of *Hyoscyamus albus*: *n*-butylamine as a potent inhibitor of the transferase both in vitro and in vivo. Plant Physiol 100:826–835

Hibi N, Higashiguchi S, Hashimoto T, Yamada Y (1994) Gene expression in tobacco low-nicotine mutants. Plant Cell 6:723–735

Jones G, Willett P, Glen RC (1995) A genetic algorithm for flexible molecular overlay and pharmacophore elucidation. J Comput Aided Mol Des 9:532–549

Jones G, Willett P, Glen RC, Leach AR, Taylor R (1997) Development and validation of a genetic algorithm for flexible docking. J Mol Biol 267:727–748

Joshi CP, Chiang VL (1998) Conserved sequence motifs in plant *S*-adenosyl-L-methionine-dependent methyltransferases. Plant Mol Biol 37:663–674

Kagan RM, Clarke S (1994) Widespread occurrence of three sequence motifs in diverse *S*-adenosylmethionine-dependent methyltransferases suggests a common structure for these enzymes. Arch Biochem Biophys 310:417–427

Korolev S, Ikeguchi Y, Skarina T, Beasley S, Arrowsmith C, Edwards A, Joachimiak A, Pegg AE, Savchenko A (2002) The crystal structure of spermidine synthase with a multisubstrate adduct inhibitor. Nat Struct Biol 9:27–31

Kozbial PZ, Mushegian AR (2005) Natural history of *S*-adenosylmethionine-binding proteins. BMC Struct Biol 5:1–26

Laemmli UK (1970) Cleavage of structural proteins during the assembly of the head of bacteriophage T4. Nature 227:680–685

Laskowski RA, MacArthur MW, Moss DS, Thornton JM (1993) PROCHECK: a program to check the stereochemical quality of protein structures. J Appl Cryst 26:283–291

Li H, Robertson AD, Jensen JH (2006) Very fast empirical prediction and rationalization of protein pKa values. Proteins: Struct Funct Bioinform 4:704–721

Liu T, Zhu P, Cheng KD, Meng C, Zhu HX (2005) Molecular cloning and expression of putrescine *N*-methyltransferase from the hairy roots of *Anisodus tanguticus*. Planta Med 71:987–989

Lounasmaa M, Tamminen T (1993) The tropane alkaloids. In: Manske RHF (ed) The alkaloids, vol 44. Academic Press, New York, pp 1–114

MacKerell AD, Bashford D, Bellott M, Dunbrack RL, Evanseck JD, Field MJ, Fischer S, Gao J, Guo H, Ha S, Joseph-McCarthy D, Kuchnir L, Kuczera K, Lau FTK, Mattos C, Michnick S, Ngo T, Nguyen DT, Prodhom B, Reiher WE, Roux B, Schlenkrich M, Smith JC, Stote R, Straub J, Watanabe M, Wiorkiewicz-Kuczera J, Yin D, Karplus M (1998) All-atom empirical potential for molecular modeling and dynamics studies of proteins. J Phys Chem B 102:3586–3616

Marcé M, Brown DS, Capell T, Figueras X, Tiburcio AF (1995) Rapid high-performance liquid chromatographic method for

the quantitation of polyamines as their dansyl derivatives: application to plant and animal tissues. J Chromatogr B Biomed Appl 666:329–335

Moffatt BA, Weretilnyk EA (2001) Sustaining *S*-adenosyl-L-methionine-dependent methyltransferase activity in plant cells. Physiol Plant 113:435–442

Nash RJ, Rothschild M, Porter EA, Watson AA, Waigh RD, Waterman PG (1993) Calystegines in Solanum and Datura species and the death's-head hawk-moth (*Acherontia atropus*). Phytochemistry 34:1281–1283

Nissink JWM, Murray C, Hartshorn M, Verdonk ML, Cole JC, Taylor R (2002) A new test set for validating predictions of protein–ligand interaction. Proteins Struct Funct Genet 49:457–471

Pellegrini E, Field MJ (2002) A generalized-born solvation model for macromolecular hybrid-potential calculations. J Phys Chem A 106:1316–1326

Riechers DE, Timko MP (1999) Structure and expression of the gene family encoding putrescine *N*-methyltransferase in *Nicotiana tabacum*: new clues to the evolutionary origin of cultivated tobacco. Plant Mol Biol 41:387–401

Sachan N, Falcone DL (2002) Wound-induced gene expression of putrescine *N*-methyltransferase in leaves of *Nicotiana tabacum*. Phytochemistry 61:797–805

Sambrook J, Fritsch EF, Maniatis T (1989) Molecular cloning. a laboratory manual 2nd edition. Cold Spring Harbour Laboratory Press, Plainview, New York

Schluckebier G, O'Gara M, Saenger W, Cheng X (1995) Universal catalytic domain structure of AdoMet-dependent methyltransferases. J Mol Biol 247:16–20

Scholl Y, Höke D, Dräger B (2001) Calystegines in *Calystegia sepium* derive from the tropane alkaloid pathway. Phytochemistry 58:883–889

Shoji T, Yamada Y, Hashimoto T (2000) Jasmonate induction of putrescine *N*-methyltransferase genes in the root of *Nicotiana sylvestris*. Plant Cell Physiol 41:831–839

Sippl MJ (1990) Calculation of conformational ensembles from potentials of mean force—an approach to the knowledge-based prediction of local structures in globular-proteins. J Mol Biol 213:859–883

Smith DD, Summers PS, Weretilnyk EA (2000) Phosphocholine synthesis in spinach: characterization of phosphoethanolamine *N*-methyltransferase. Physiol Plant 108:286–294

Stenzel O, Teuber M, Dräger B (2006) Putrescine *N*-methyltransferase in *Solanum tuberosum* L., a calystegine-forming plant . Planta 223:200–212

Suzuki K, Yamada Y, Hashimoto T (1999) Expression of *Atropa belladonna* putrescine *N*-methyltransferase gene in root pericycle. Plant Cell Physiol 40:289–297

Verdonk ML, Cole JC, Hartshorn MJ, Murray CW, Taylor RD (2003) Improved protein–ligand docking using GOLD. Proteins Struct Funct Genet 52:609–623

Walton NJ, Peerless A-CJ, Robins RJ, Rhodes M-JC, Boswell HD, Robins DJ (1994) Purification and properties of putrescine *N*-methyltransferase from transformed roots of *Datura stramonium* L. Planta 193:9–15

Winz RA, Baldwin IT (2001) Molecular interactions between the specialist herbivore *Manduca sexta* (Lepidoptera, Sphingidae) and its natural host *Nicotiana attenuata*. IV. Insect-induced ethylene reduces jasmonate-induced nicotine accumulation by regulating putrescine *N*-methyltransferase transcripts. Plant Physiol 125:2189–2202

Yamaguchi H, Nishimoto K (1965) Alkaloids of the root of *Physalis alkekengi.* I. Isolation of 3a-(tigloyloxy)tropane. Chem Pharm Bull 13:217–220

Yoon SO, Lee YS, Lee SH, Cho YD (2000) Polyamine synthesis in plants: isolation and characterization of spermidine synthase from soybean *(Glycine max)* axes. Biochim Biophys Acta 1475:17–26

Zhang ZP, Baldwin IT (1997) Transport of (2-^{14}C)jasmonic acid from leaves to roots mimics wound-induced changes in endogenous jasmonic acid pools in *Nicotiana sylvestris*. Planta 203:436–441

Zubieta C, He XZ, Dixon RA, Noel JP (2001) Structures of two natural product methyltransferases reveal the basis for substrate specificity in plant *O*-methyltransferases. Nat Struct Biol 8:271–279